Study of the substructure of two high-mass molecular clumps

N.L. Isequilla[1], A.D. Marinelli[1] & M.E. Ortega[1]
[1] *Instituto de Astronomía y Física del Espacio, CONICET–UBA, Argentina*

Received: 09 February 2024 / Accepted: 17 July 2024

Resumen / El estudio de la formación de las estrellas de alta masa incluye la caracterización de la estructura interna de los grumos moleculares de alta masa. En este trabajo se presenta un estudio de la subestructura de las fuentes ATLASGAL G020.761−00.062 y G033.133−00.092, a partir de la base de datos del interferómetro Atacama Large Millimeter Array (ALMA) y de observaciones propias realizadas con el Karl G. Jansky Very Large Array (JVLA). Ambos grumos moleculares de alta masa muestran evidencia de fragmentación con la presencia de varios núcleos moleculares en su interior, algunos de ellos activos. La detección de fuentes de radio podría sugerir la presencia de regiones HII jóvenes embebidas en ambos grumos mostrando que la formación estelar de alta masa ha tenido lugar en su interior. Teniendo en cuenta las moléculas detectadas en dirección a ambos grumos moleculares, en un trabajo futuro se caracterizará el estado evolutivo y la masa de los diferentes fragmentos observados.

Abstract / The study of the formation of high-mass stars includes the characterisation of the internal structure of high-mass molecular clumps. This work presents a study of the substructure of the sources ATLASGAL G020.761−00.062 and G033.133−00.092, based on data from archival of the Atacama Large Millimeter Array (ALMA) interferometer and own observations carried out with the Karl G. Jansky Very Large Array (JVLA). Both massive molecular clumps show evidence of fragmentation with the presence of several molecular cores, some of them active. The detection of a radio source could suggest the presence of young HII regions embedded in both clumps showing that high-mass star formation has taken place inside them. From the different molecules detected towards the molecular cores, it is intended, in the future, to characterise the evolutionary stage and mass of the different fragments.

Keywords / stars: formation — ISM: molecules — stars: protostars

1. Introduction

Star formation proceeds in dense regions of the molecular clouds. In particular, the formation of massive stars (>8 $M_\odot$) occurs in massive molecular clumps. These molecular clumps fragment and collapse gravitationally, giving rise to multiple molecular cores. These cores can be massive enough to form massive stars (McKee & Tan, 2002), or instead, they may generate low-mass cores that eventually form massive stars through competitive accretion (Bonnell, 2008; Sanhueza et al., 2019). Therefore, the mass distribution and number of cores detected depend on the process that regulates fragmentation, as well as the evolutionary stage of the cloud (Moscadelli et al., 2021; Palau et al., 2018; Kainulainen et al., 2013). The characterisation of molecular cores embedded in massive clumps is important for understanding the formation of high-mass stars.

We present a continuation of the study carried out by Marinelli et al. (2022) of the molecular clumps AGAL G020.761−00.062 (hereafter G20.76) and AGAL G033.133−00.092 (hereafter G33.13). We used high angular resolution and sensitivity data, obtained from the Atacama Large Millimeter Array (ALMA) archival database, and our own radio continuum observations from the Karl G. Jansky Very Large Array (JVLA).* Marinelli et al. (2022) showed evidence of fragmentation towards both molecular clumps. In particular, from the CH_3CN emission, detected towards some of the fragments, the authors estimated temperatures above 100 K for some of the cores, which indicate that active star formation is occurring inside them (Remijan et al., 2004). Moreover, we have detected many more interesting molecules towards these cores, characterizing them through these molecules will give us a better understanding of the processes occurring in the region (to be published in a forthcoming paper, Isequilla et al., in prep). Therefore, as an example, we present the spatial distribution of one of them ($C^{17}O$).

On the other hand, we present images of radio continuum at 10 GHz from our JVLA observations to unveil the presence of more evolved massive sources, which may have already begun to ionise their surroundings as compact HII regions.

In this work, we present a preliminary characterisation of two massive dust condensations at clump (G20.76 and G33.13) and core scale as part of a larger

*The NRAO is a facility of the National Science Foundation operated under cooperative agreement by Associated Universities, Inc.

✉ *Contact* / nisequilla@iafe.uba.ar Research article study aimed at determining the evolutionary state and mass of all the molecular cores in the region. This is in order to contrast the two main scenarios of high-mass star formation.

2. Data

Data cubes were obtained from the ALMA Science Archive**, project 2015.1.01312 (PI: Fuller, G). The single pointing observations for the targets were carried out using the following telescope configuration with L5BL/L80BL(m): 42.6/221.3, in the 12 m array. The observed frequency range and the spectral resolution are 224.24 – 242.75 GHz (band 6) and 1.3 MHz, respectively. The angular resolution of this dataset is about $0''.7$. The rms noise is 1.5 and 0.05 mJy beam^{-1} for the line emission and the continuum, respectively.

Observations with the JVLA*** interferometer were carried out at X-band, covering the frequency range from 8 to 12 GHz. The observations were taken on May 18, 2022, in the A configuration (Project 22A-063, PI: Ortega, M.). The rms noise level and synthesised beam obtained were 6 μJy beam^{-1} and $0.''6 \times 0.''2$ towards G20.76, and 0.1 mJy beam^{-1} and $0.''4 \times 0.''2$ towards G33.13. Both ALMA and JVLA data were calibrated and analysed using the Common Astronomy Software Applications package (CASA, McMullin et al., 2007, version 4.7.2).

Additionally, we used 870 μm data extracted from ATLASGAL (Schuller et al., 2010), and *Spitzer* data at 8 and 24 μm extracted from GLIMPSE (Benjamin et al., 2003), and MIPSGAL (Carey et al., 2009), respectively.

3. Characterizing the ATLASGAL sources and their substructure

Figure 1 shows three-color images towards the G20.76 (left panel) and G33.13 (right panel) sources. These images show the *Spitzer* data at 8 and 24 μm in green and red, respectively, and JVLA data at 1.4 GHz in blue. The white contours represent the ATLASGAL emission at 870 μm. Both images show the presence of several dust condensations at 870 μm. The complexes G20.76 and G33.13 have associated systemic velocities of approximately 57 km s^{-1} and 76 km s^{-1} (Wienen et al., 2012), corresponding to kinematic distances of about 4.12 kpc and 9.37 kpc, respectively (Wienen et al., 2015).

From the dust continuum emission at 870 μm extracted from ATLASGAL catalogues, we estimated the mass of the two molecular clumps, following Kauffmann et al. (2008)

$$\mathrm{M_{gas}} = 0.12\ \mathrm{M_\odot} \left[\exp\left(\frac{1.439}{(\lambda/\mathrm{mm})(\mathrm{T_{dust}}/10\ \mathrm{K})}\right) - 1\right] \times \left(\frac{\kappa_\nu}{0.01\ \mathrm{cm^2\ g^{-1}}}\right)^{-1} \left(\frac{\mathrm{S}_\nu}{\mathrm{Jy}}\right) \left(\frac{\mathrm{d}}{100\ \mathrm{pc}}\right)^2 \left(\frac{\lambda}{\mathrm{mm}}\right)^3.$$

For κ_ν, the dust opacity per gram of matter at λ = 870 μm, we adopted the value 0.0185 cm^{2}g^{-1} (Csengeri et al., 2017). Assuming a typical dust temperature $\mathrm{T_{dust}}$=20 K (Wienen et al., 2012), along with integrated flux densities S_v =1.76 Jy and 8.08 Jy for G20.76 and G33.13, respectively, as estimated by Csengeri et al. (2014), we derived masses of 173 $\pm$ 51 $\mathrm{M_\odot}$ for the clump G20.76 at a distance d= 4.12 kpc and 4106 $\pm$ 1231 $\mathrm{M_\odot}$ for the clump G33.13 at a distance d= 9.37 kpc. These results confirm that both ATLASGAL sources are indeed massive molecular clumps, which makes them interesting objects for studying the fragmentation and formation of high-mass stars.

It has previously been mentioned that Marinelli et al. (2022) found evidence of fragmentation towards both molecular clumps. As part of a continuation of that work, and based on a preliminary analysis of ALMA data, we have found many interesting molecules towards the molecular cores in which both clumps G20.76 and G33.13 have been fragmented. These molecular lines provide crucial information about the physical and chemical conditions of the cores embedded in the molecular clumps. For instance, we have detected molecules such as CN, $C^{17}O$, $C^{34}S$, CH_3OH, H_2CO, which exhibit extended emission beyond the cores, along with other molecules like HDO, CH_3CN (analysed in Marinelli et al., 2022), CH_3CCN, HC_3N, which show localised emission towards specific cores. In this work, we only show the spatial distribution of the $C^{17}O$ molecule, which is one of the most common molecules in the interstellar medium.

Figure 2 shows in grayscale the integrated emission of the $C^{17}O$ J=2–1 line towards G20.76 (top panel) and G33.13 (bottom panel). The green contours represent the ALMA continuum emission at 1.3 mm. The molecular cores, in which both clumps have fragmented, are labelled with mm#. Figure 2 (top panel) exhibits a shell-like morphology extending to the south of the dust cores's complex. This shell-like feature encompasses the position of the cores mm1 and mm2, while core mm3 seems to be outside the structure. Figure 2 (bottom panel) displays the $C^{17}O$ J=2–1 emission, revealing two prominent molecular condensations coinciding with the positions of the dust cores mm3 and mm4. Additionally, extended emission surrounding all the cores is visible.

Unlike the CH_3CN (J=13–12) line emission, which traces denser and hotter (E_u above 100 K)**** gas towards molecular hot cores (see Marinelli et al., 2022), the $C^{17}O$ (J=2–1) transition traces less dense and cooler ($\mathrm{E}_u \sim$ 20 K) gas of the external layer of the envelope in which the cores are embedded (Fontani et al., 2005). The kinematic analysis of the $C^{17}O$ (J=2–1) emission helps us to investigate how the fragmentation processes have occurred inside the molecular clumps, given that this molecule can trace the ambient gas connecting the cores that remains after the process of fragmentation (e.g. filaments).

Figure 3 shows, in grayscale, the JVLA radio continuum emission at 10 GHz towards G20.76 (top panel) and G33.13 (bottom panel), which were previously cat-

**http://almascience.eso.org/aq/

***https://data.nrao.edu

****Excitation energy of the upper level.

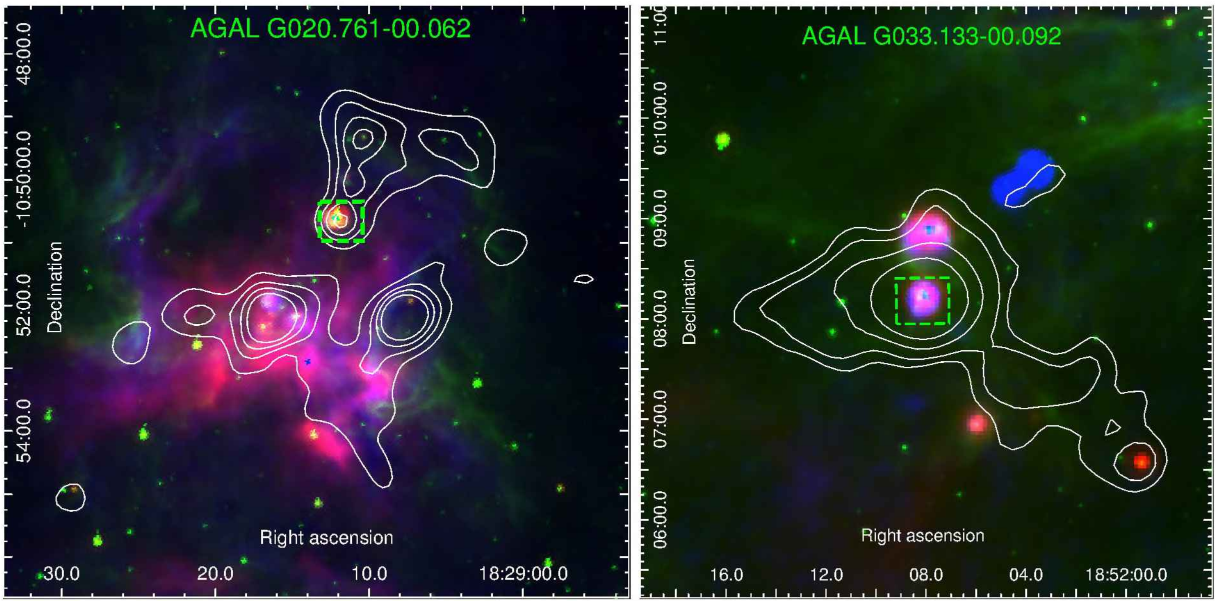

Fig. 1. A three color image with *Spitzer* data at 8 and 24 μm in green and red, respectively, and JVLA data at 1.4 GHz in blue. The white contours represent the ATLASGAL continuum emission at 870 μm. Levels are at 0.25 (3σ), 0.45, 0.65, and 0.9 Jy beam^{-1} for G20.76 (left panel) and at 0.11 (3σ), 0.19, 0.4, and 0.8 Jy beam^{-1} for G33.13 (right panel). The green squares highlight the regions studied in this work.

alogued as radio sources according to the survey carried out by Purcell et al. (2013). In G20.76 it can be appreciated a radio source towards the south of the molecular core complex. The radio source exhibits extended structure and it is associated with what would appear to be the remains of an ancient molecular core. We are investigating the connection between this radio source and the $C^{17}O$ molecular shell (Isequilla et al., in prep).

In G33.13 appears an intense radio source located between the molecular cores mm2 and mm3. Conspicuous extended emission seems to extend eastwards towards the position of the core mm2, suggesting a spatial connection between this radio source and the distribution of molecular gas. However, further analysis is required to confirm this possibility.

Subsequent studies of spectral index towards these radio sources will allow us to determine their nature, however given their morphology it is reasonable to assume that the radio continuum emission is ionised gas linked to young and compact HII regions. If this is the case, they would be evidence that high-mass star formation has taken place in both massive molecular clumps.

4. Summary and future work

We presented a preliminary study of the internal structure of the ATLASGAL sources G20.76 and G33.13 (massive clumps) based on the analysis of high resolution and sensitivity archival ALMA data and new JVLA observations. The main results are:

- Both ATLASGAL sources are massive dust clumps ~ 173 $M_\odot$ and ~ 4106 $M_\odot$ for G20.76 and G33.13, respectively, which makes them interesting objects for analysing the fragmentation processes and the subsequent high-mass star formation,
- The ALMA continuum emission at 1.3 mm shows evidence of fragmentation towards both clumps,
- The $C^{17}O$ (J=2–1) integrated emission map towards G20.76 shows a fragmented shell-like structure extending to the south of the dust cores's complex,
- The JVLA radio continuum emission maps at 10 GHz suggest the presence of two young and compact HII regions, one within each clump, indicating that high-mass star formation has already occurred within both,
- The JVLA radio source towards G20.76 could be related to the molecular shell-like feature found in the $C^{17}O$ (J=2–1) emission,
- The JVLA radio source towards G20.76 seems to be related to the remains of an ancient core (the more evolved one in the clump) weakly detected with our ALMA observations, while the JVLA radio source towards G33.13 seems to be related to the core mm2. However, a more in-depth study is required to be conclusive.

The study will continue with a comprehensive characterisation of all the molecular cores identified in both clumps, based on a deep analysis of the ALMA (line and continuum) and JVLA observations (continuum), and complemented with near-infrared public data. The analysis of the molecular lines detected towards both clumps will allow us to determine the evolutive stage and the mass of the still present molecular cores. The fundamental objective of this study will be to contrast the two main scenarios of high-mass star formation: monolithic accretion and competitive collapse.

Acknowledgements: N.L.I and M.O. are members of the Carrera del Investigador Científico of CONICET, Argentina. A.M. is a doctoral fellows of CONICET, Argentina. This work was partially supported by the Argentinian grants PIP 2021 11220200100012

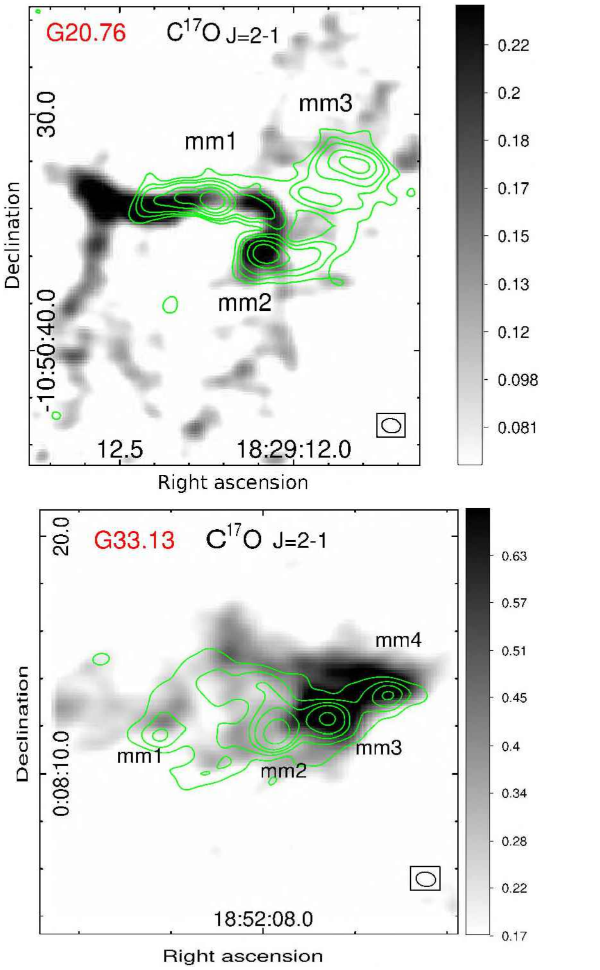

Fig. 2. Grayscale shows the zero moment maps of $C^{17}O$ (J=2–1) towards G20.76 (top panel) and G33.13 (bottom panel) integrated between 52 and 62 km s^{-1} and between 71 and 81 km s^{-1}, respectively. The grayscale is in Jy beam^{-1} km s^{-1}. The green contours represent the ALMA continuum emission at 1.3 mm. Levels are at 0.7, 1.2, 1.9, 4, 7, and 13 mJy beam^{-1} and at 3, 6.7, 12, 20, and 50 mJy beam^{-1} for G20.76 and G33.13, respectively. The labels mm# indicate the core names. The beams are showed at the bottom right corner.

and PICT 2021-GRF-TII-00061 awarded by CONICET and ANPCYT.

References

Benjamin R.A., et al., 2003, PASP, 115, 953
Bonnell I.A., 2008, J.H. Knapen, T.J. Mahoney, A. Vazdekis (Eds.), *Pathways Through an Eclectic Universe*, *Astronomical Society of the Pacific Conference Series*, vol. 390, 26
Carey S.J., et al., 2009, PASP, 121, 76
Csengeri T., et al., 2014, A&A, 565, A75
Csengeri T., et al., 2017, A&A, 601, A60
Fontani F., et al., 2005, A&A, 432, 921
Kainulainen J., et al., 2013, A&A, 557, A120
Kauffmann J., et al., 2008, A&A, 487, 993
Marinelli A.D., et al., 2022, Boletin de la Asociacion Argentina de Astronomia, Argentina, 63, 146

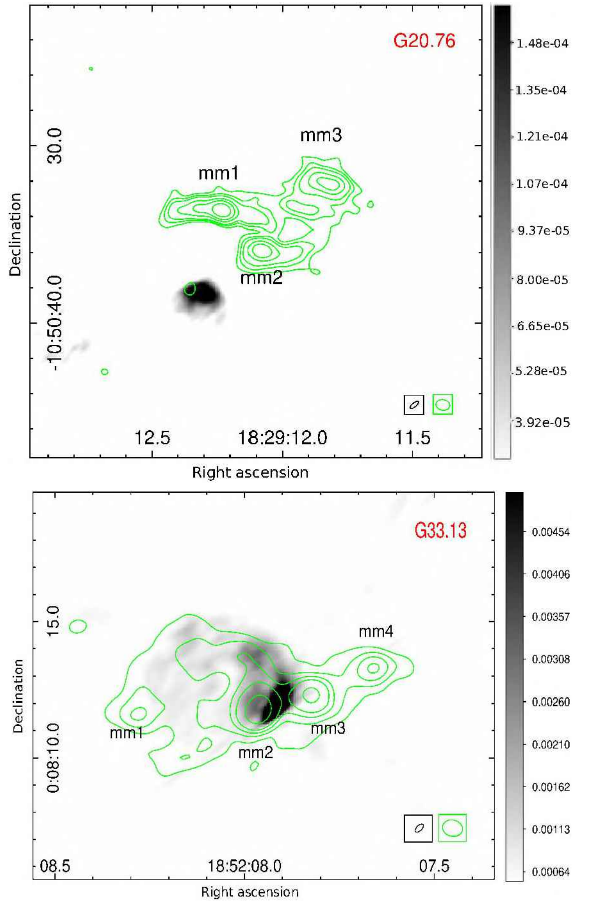

Fig. 3. Grayscale radio images showing the two sources detected with the JVLA at 10 GHz: G20.76 (top) and G33.13 (bottom). The green contours (the same as in Fig. 2) trace the dust continuum emission at 1.3 mm. The beams are indicated in the bottom right corner of each image, in black JVLA and green ALMA.

McKee C.F., Tan J.C., 2002, Nature, 416, 59
McMullin J.P., et al., 2007, R.A. Shaw, F. Hill, D.J. Bell (Eds.), *Astronomical Data Analysis Software and Systems XVI*, *Astronomical Society of the Pacific Conference Series*, vol. 376, 127
Moscadelli L., et al., 2021, A&A, 647, A114
Palau A., et al., 2018, ApJ, 855, 24
Purcell C.R., et al., 2013, ApJS, 205, 1
Remijan A., et al., 2004, ApJ, 606, 917
Sanhueza P., et al., 2019, ApJ, 886, 102
Schuller F., et al., 2010, The Messenger, 141, 20
Wienen M., et al., 2012, A&A, 544, A146
Wienen M., et al., 2015, A&A, 579, A91